

Static Radical Stiffness and Contact Behavior of Non-pneumatic Mechanical Elastic Wheel

ZANG Ligu^{1,2}, ZHAO Youqun^{2*}, SUN Haiyan¹, LIN Fen²

1. School of Automotive and Rail Transit, Nanjing Institute of Technology, Nanjing 211167, P. R. China;

2. College of Energy and Power Engineering, Nanjing University of Aeronautics and Astronautics, Nanjing 210016, P. R. China

(Received 22 November 2017; revised 6 May 2018; accepted 28 May 2019)

Abstract: Conventional pneumatic tires exhibit disadvantages such as puncture, blowout at high speed, pressure maintenance, etc. Owing to these structural inevitable weaknesses, non-pneumatic tires have been developed and are investigated. A non-pneumatic mechanical elastic wheel (NPMEW) is introduced and investigated as a function of static radical stiffness characteristics and contact behavior. A bench test method is utilized to improve the riding comfort and the traction traffic ability of NPMEW based on tire characteristics test rig, and the static radical stiffness characteristics and the contact behavior of NPMEW are compared with that of an insert supporting run-flat tire (ISRFT). The vertical force-deformation curves and deformed shapes and contact areas of the NPMEW and ISRFT are obtained using a set of vertical loads. The contact behavior is evaluated using extracted geometrical and mechanical feature parameters of the two tires. The results indicate that the NPMEW appears to exhibit considerably high radical stiffness, and the numerical value is dependent on the mechanical characteristic of the flexible tire body and hinge units. NPMEW demonstrates more uniform contact pressure than ISRFT within a certain loading range, and it can efficiently mitigate the problem of stress concentration in ISRFT shoulder under heavy load and enhance the wear resistance and ground grip performances.

Key words: vehicles; non-pneumatic mechanical elastic wheel; run-flat tire; radical stiffness; contact behavior

CLC number: U463.341 **Document code:** A **Article ID:** 1005-1120(2019)04-0663-12

0 Introduction

Vehicle tires are the only component that directly contacts with the ground, and the interface between the vehicle and the highway provides all forces and moments to support a vehicle load. It also absorbs road irregularities, which provides a major effect on riding comfort, handling stability, tire wear, and noise^[1-2]. The tire stiffness characteristics and contact behavior exhibit significant effect on passengers' comfort, vehicle handling, wear, and noise. Moreover, it has been an important problem in case of tire design. Improper stiffness and contact pressure, excessively high or excessively low, result in rapid wear of tread, poor ride comfort of passen-

gers, difficulty in tire control, affecting vehicle handling stability, producing noise, etc.^[3-5].

The conventional pneumatic tires have been the dominant design and been in use for more than 100 years owing to its low vertical stiffness, low contact pressure, and low mass^[1,6]. However, the pneumatic tire has several disadvantages such as puncture, blowout at high speed, requirement of pressure maintenance, etc. Besides, tire flattening results in crown deformation, which is difficult to be controlled and would induce uneven contact pressure distribution, energy loss, and other problems. Therefore, several tire engineers and research institutions have attempted to develop non-pneumatic tires or run-flat tires to solve these inherent prob-

*Corresponding author, E-mail address: yqzhao@nuaa.edu.cn.

How to cite this article: ZANG Ligu, ZHAO Youqun, SUN Haiyan, et al. Static Radical Stiffness and Contact Behavior of Non-pneumatic Mechanical Elastic Wheel[J]. Transactions of Nanjing University of Aeronautics and Astronautics, 2019, 36(4):663-674.

<http://dx.doi.org/10.16356/j.1005-1120.2019.04.013>

lems. Certain types of non-pneumatic tire are being developed, such as hexagonal honeycombs non-pneumatic tire^[3,5,7], and non-pneumatic Tweel, which is composed of three major systems, a critical shear beam, two inextensible membranes, deformable spokes^[6,8-9], and mechanical elastic wheel^[10-12]. Besides, certain types of non-pneumatic tire based on pneumatic tire, which enable vehicles to be driven on the road at normal speed for limited distances even after puncture occurs, have been developed since the concept was introduced, and the representatives are the self-supporting tires with an interior supporting ring and sidewall reinforced run-flat tire^[13-14].

Non-pneumatic mechanical elastic wheel is a novel non-pneumatic tire. The mechanical characteristics of the wheel, including its driving force model^[15], steady-state and transient dynamic characteristics^[16-18], grounding characteristics^[19] and camber performance^[20] have been studied and its few advantages over a pneumatic tire in some respects were presented. For a variety of non-pneumatic tires, having as superior elasticity property including conventional pneumatic tires is important. This is also the primary design problem to realize the pneumatic tire replacement on pneumatic tire. For the mechanics, elastic properties of tire reflect different direction for tire stiffness. The interface between the wheel and the road surface provides all forces and moments for off-road vehicle with mechanical elastic wheel. The radial stiffness and contact behavior of the wheel exhibit significant effect on passengers' comfort, vehicle handling, wear, and noise.

Radial stiffness is one of the basic mechanical parameters of tire, which has an important impact on the vertical vibration of tire and various driving performances of vehicle. The radial stiffness of pneumatic tire is related to the width of tire section, rim diameter, pressure, and other factors. The overall performance of pneumatic tire can be improved by optimizing these parameters in design. For non-pneumatic elastic wheel, the radial stiffness mainly depends on the initial design parameters. The radial stiffness of wheels should not only satisfy the requirement of small contact patch when driving on

hard road surface to reduce rolling resistance, but also satisfy the requirement of large contact patch when driving on soft and muddy road surface to improve adhesion performance. Therefore, it is very important to study the regularity between radical stiffness and contact patch.

A non-pneumatic mechanical elastic wheel (NPMEW) is investigated here as a function of static radical stiffness characteristics and contact pressure to improve vehicle traction trafficability and off-road reliability. In a series of our previous studies, we had constructed the finite element model of NPMEW, and systematically studied its mechanical properties and traction trafficability characteristic using theoretical and experimental methods^[10-12,21-23]. A bench test method was utilized to investigate the static radical stiffness characteristics and contact behavior of NPMEW based on a self-developed tire static characteristic test bench, and were compared with that of an insert supporting run-flat tire (ISRFT). The vertical force-deflection curves and deformed shapes and footprint of the NPMEW and ISRFT were obtained using a set of vertical loads. The contact pressure distribution of the NPMEW and ISRFT were obtained using a pressure sensitive film laid on the platform of the tire characteristics test rig. This study proposes the change laws and effective factors of radical stiffness and contact pressure distribution to enhance the passenger comfort and the durability of the NPMEW by optimizing the structure and parameters.

1 Structure and Principle of NPMEW

1.1 Structure of NPMEW

The NPMEW does not follow the traditional design method of vehicle travelling system, which is composed of separate components including tires and wheels. The NPMEW includes flexible tire body, hinge unit, suspension hub, and other components, as shown in Fig.1. It adopts a hinge unit to connect the flexible tire body and the suspension

hub. This non-pneumatic structure ensures that the NPMEW avoids puncture, blowout at high speed, etc. Among them, the flexible tire body is composed of snap ring, combined elastic ring, and belt layer.

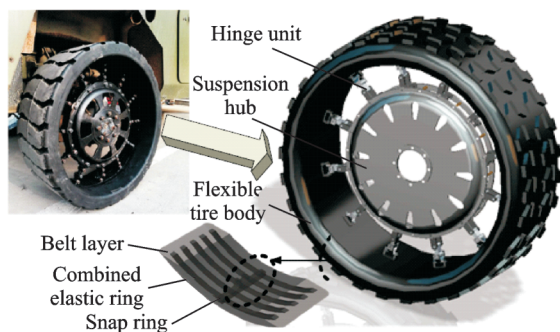


Fig.1 Non-pneumatic mechanical elastic wheel structure

The hinge unit connecting the flexible tire body and suspension hub is comprised of three hinges. The length of the hinge unit is slightly longer than the radial distance between the flexible tire body and suspension hub. The hinges are connected using pin rolls, which develops a revolute pair. The suspension hub is hung on the flexible tire body circular-distributed hinge unit, thus it is also called suspension hub. Because the hinge unit can only sustain tension, the hinge unit at the bottom of NPMEW is curved. Hinge 1 can move laterally within a certain angle, which ensures satisfactory lateral stability and lateral stiffness.

1.2 Load-carrying mechanism of NPMEW

Two types of load-carrying mechanisms exist regarding the present wheels: bottom loaders and top loaders^[6]. Refer to Fig.2 for a graphical comparison between the bottom loaders and top loaders.

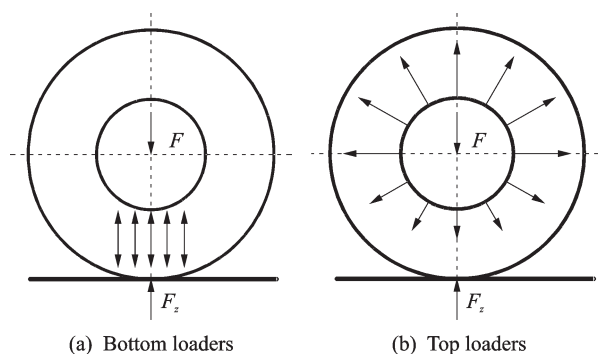


Fig.2 Load-carrying mechanism for present wheels

The typical structure of the bottom loaders is rigid wheel, which carry the load through direct compression from the contact area to the wheel suspension hub, as shown in Fig.2(a). At any instant, only a small portion of the wheel is involved in carrying the load, resulting in an inherently poor efficiency in terms of load capacity per unit mass. The typical structure of the top loaders is the tensioned spoke wheel. The vector sum of the spoke tensions determines the load carried by the wheel, as shown in Fig.2(b). At any bearing load instant, all of the spokes are involved in carrying the load, thus the load capacity per unit mass of this structure is significantly increased.

The load-carrying mechanism of pneumatic tires is similar to that of the tensioned spoke wheel. The spokes are represented via continuous rubber tire, thus its load capacity per unit mass is similar to that of the tensioned spoke wheel.

The load-carrying mechanism of NPMEW is shown in Fig.3, and the load-carrying is defined as suspension hub loaders. The vector sum of the tensions of the hinge units determines the load carried by the NPMEW. The load-carrying is also similar to top loaders except for the hinge units at the bottom of the NPMEW.

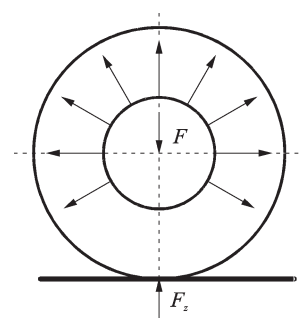


Fig.3 Load-carrying mechanism of NPMEW

When the NPMEW is under static vertical load, the outer flexible tire body is deformed and the grounded area is flattened. In addition to those near the contact area, the rest of the hinge units are under tension, and the suspension hub in the middle is hung on the outer flexible tire body. It exhibits high load capacity per unit mass similar to top loaders, and can guarantee sufficient contact deforma-

tion between the wheel and the ground, so as to make the wheel possess satisfactory adhesion performance.

1.3 Radical stiffness and contact patch

With reference to the definition of the pneumatic tire stiffness, the radial stiffness, lateral stiffness, and torsional stiffness of NPMEW are defined^[24]. The radial stiffness is the ratio of radial force and radial deformation. In addition, the flexible tire body is defined as the structure without suspension hub and hinges. The stiffness of the flexible tire body is the same as that of the mechanical elastic wheel. The definition of hinge stiffness is the ratio of strain and deformation.

The deformation of NPMEW perpendicular to the plane of the car wheel shaft under vertical load is shown in Fig.4.

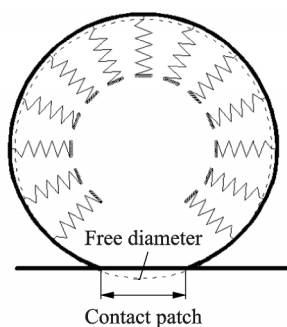


Fig.4 Deformation under vertical load

Based on wheel structure and stress analysis, the radial stiffness depends primarily on the structural mechanical characteristics of the flexible tire body and the hinge. A positive correlation exists between the stiffness of NPMEW and the stiffness of flexible tire body. The flexible tire body stiffness depends primarily on the elastic ring stiffness, a number of combinations of the elastic ring and structure dimensions of the flexible tire body etc. For hinge units, the material properties and quantity have significant effect on the stiffness characteristics of NPMEW.

To better understand the relationship between radical stiffness and contact patch, the equivalent acting force was applied to the bottom of NPMEW with fixed axle. Compared with the free state, the upper portion of the flexible tire body was expanded and the bottom portion deformed in the pavement

contact area, as shown in Fig. 5. When the hinge units act as springs, the outer flexible tire body can easily increase in diameter and the contact patch can shorten, which is a case of low stiffness. If the hinge units act as stiff springs, it is difficult for the flexible tire body to increase the diameter and a considerable amount of the extra length should be included into the contact length, which is the high stiffness case. Fig. 5 provides a schematic representation of these two cases. The contact pressure and the stiffness of the wheel are uncoupled.

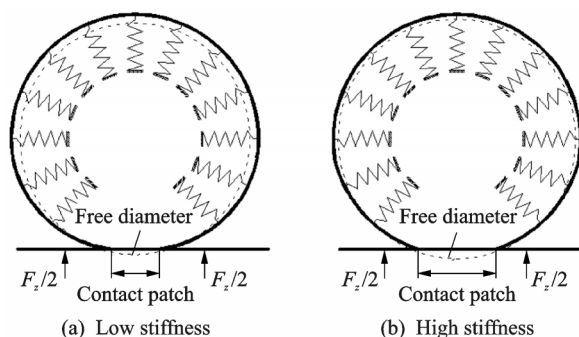


Fig.5 Low stiffness and high stiffness

2 Static Radical Stiffness and Contact Behavior Tests

2.1 Static radical stiffness test

The radical stiffness and contact behavior tests were conducted on the self-developed tire characteristic test rig, which possessed two types of loading method, applying load to the top and the suspension hub. The test rig is primarily composed of hydraulic loading device, bearing plate, positioning guide device, measuring device, etc. The hydraulic loading device can use any stable vertical load regarding various tires to simulate the actual loading. To study the bearing deformation mechanism of the NPMEW, two loading modes are designed. The load is respectively applied to the top of the tire and wheel suspension hub. Pressure sensitive films are spread on the bearing plate with respect to the contact patch and the contact pressure distribution. Fig.6 shows the ISRFT applied load to the hub. The gate apparatus of the tire characteristic test rig ensures vertical load and measures the deformation



Fig.6 Tire characteristic test rig

of the NPMEW and ISRFT under a group of load.

The NPMEW and ISRFT were marked evenly with 12 points along the circumference before the experiment begins, and measuring the distance between two points in the diameter direction could determine the wheel deformation under the load. Deformation path map could be obtained using point depiction method. Two typical types working conditions for NPMEW were measured, as shown in Fig.7; in one condition, the hinge unit is in the middle of the pavement contact area, and in the other condition, the gap between two hinge units is in the middle of the pavement contact area.

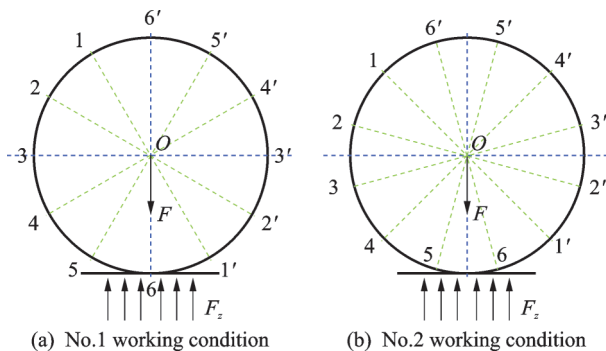


Fig.7 Two typical types of loading conditions for NPMEW

For a better understanding of the radical stiffness characteristics, the flexible tire body was also applied load to the top based on tire characteristics test rig. The flexible tire body is the structure where all hinge units and the suspension hub of the NPMEW are dismantled. It is defined in Section 1.3.

2.2 Static contact behavior test

The primary test methods of tire contact behavior are pressure plate method, pressure sensor method, pressure sensitive film method, and optical ab-

sorption method^[25]. The measuring process using the pressure sensitive film method is simple and rapid and the measurement results, both visual and digital, are accurate. Thus, the method is adopted to study the static contact behavior.

The contact pressure distribution of the NPMEW and ISRFT were obtained using a pressure sensitive film laid on the bearing plate of the tire characteristics test rig, as shown in Fig.8. When tires are in contact with pavement, different stress distributions will occur on the contact patch. Normal and tangential stresses exist at any point in the contact patch. The magnitude and direction of stress distribution depend on the load, motion state, structure and road friction coefficient. In this experiment, only normal force is considered. Two layers of pressure sensitive film, A and B, inserted between tire and pavement. In the contact patch, the pressure sensitive film will display images of different densities according to the magnitude of pressure. Images of different densities represent the magnitude of the contact pressure.

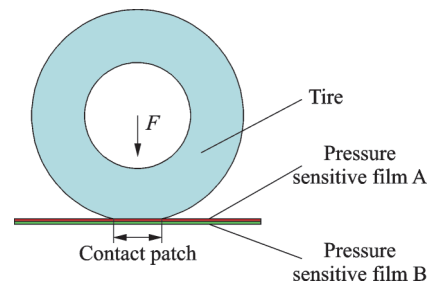


Fig.8 Mechanism of pressure sensitive film method

Before the test, the NPMEW and ISRFT were preprocessed according to the relevant China national standards, and the rig was calibrated. Tire pressure of ISRFT was readjusted to the standard pressure. Subsequently, the tire was fixed on the rig through the axle; the sensitive film was placed between the tire and the platform of the tire characteristics test rig. The platform should be smooth and satisfy the following conditions: possessing sufficiently large contact patch, and sufficient stiffness resisting deformation of configuration under maximum load. A set of vertical loads was applied to the

specified value under sustainable speed, which should ensure that pressure sensitive film does not wrinkle.

To make the results be well correlated, the geometrical parameters of NPMEW in this test are the same as that of ISRFT. The maximum mass of ISRFT is 1 750 kg, and the rated air pressure is 350 kPa.

3 Experimental Results

3.1 Static radical stiffness behavior

A comparison of the load deformation behavior of the NPMEW at No.1 condition is shown in Fig.9. The bottom portion of the NPMEW is deformed to be flat with respect to the contact area. The load deformation behavior of the flexible tire body also can be determined by the other loading method at No.1 condition, applying load to the top based on tire characteristics test rig, as shown in Fig.9(b).

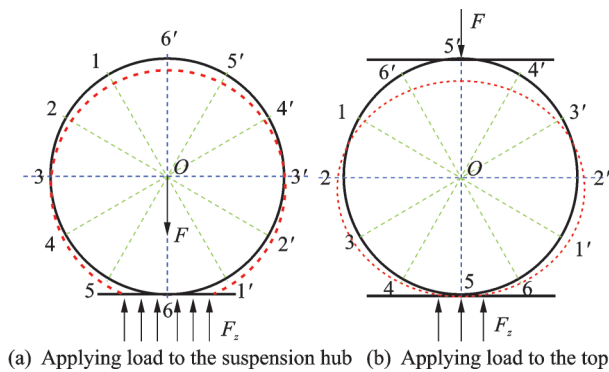
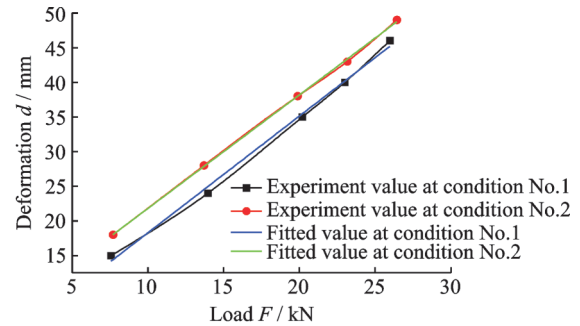
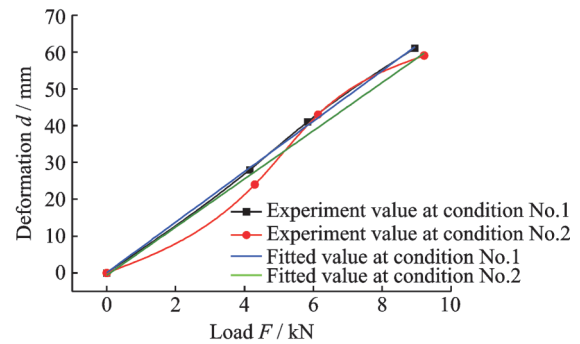


Fig.9 Load deformation behavior of NPMEW and flexible tire body at condition No.1

Typical load deformation curves of the NPMEW and flexible tire body were obtained based on two typical types of working conditions as shown in Fig.10, and using linear regression technology to fit. The load-deformation approximates to a straight line in certain range of vertical load as shown in Fig.10(a). Thus, the average radial stiffness of the NPMEW can be calculated. The average radial stiffness at working condition No.1 is 593.06 N/mm and that at working condition No.2 is 602.60 N/mm. Empirical data indicate that the radial stiffness



(a) Experiment and fitted load deformation curves of NPMEW



(b) Experiment and fitted load deformation curves of flexible tire body

Fig.10 Load deformation curves of NPMEW and flexible tire body

of the NPMEW is virtually identical, and the percentage of difference between working conditions No.1 and No.2 is 1.6%.

Compared with the curve at working condition No.1, where load-deformation also approximates to a straight line, the load-deformation curve of the flexible tire body at working condition No.2 appears to be nonlinear, and linear regression technology is used to fit the curve as shown in Fig.10(b). The average radial stiffness of the flexible tire body at working condition No.1 is 146.29 N/mm, and that at working condition No.2 is 150.68 N/mm. The average relative error between the values of working conditions No.1 and No.2 is 3%.

With no tensions in the hinge units, the load deformation of the flexible tire body is less evident than that of the NPMEW under the same vertical load. The experimental results indicate that the hinge units have an important effect on the radical stiffness behavior of the NPMEW.

The deformation curves of the ISRFT are obtained using method of applying load to the hub, as shown in Fig.11. The experimental result exhibited

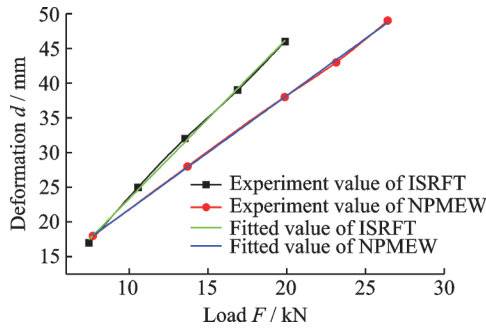


Fig.11 Load deformation curves of NPMEW and ISRFT

an exceptionally satisfactory linear relationship between the vertical load and the deformation. The average radial stiffness of the ISRFT is 433.63 N/mm, and that value is less than the average value of NPMEW, but larger than the value of flexible tire body.

The rolling resistance of NPMEW is less than that of ISRFT because it can maintain suitable circular degree as the vehicle drives on rough roads, which results in poor riding comfort. To replace the pneumatic tire, the NPMEW stiffness characteris-

tics require further optimization and to be matched with the suspension system and the entire vehicle dynamics parameters.

The residual sum of square (RSS), correlation coefficient (Pearson's ratio), adjusted determination coefficient (Adj. R -square), and standard error (σ) were extracted to evaluate the goodness of fit and the regular characteristics of load deformation curve, depicted in Table 1. The load deformation curves indicate a satisfactory linear relationship from the aspect of Pearson's ratio and Adj. R -square under permissible load range, and the RSS at working condition No.2 is less than that at No.1, indicating a good fitting degree.

Fitting parameters of the flexible tire body and the ISRFT are shown in Table 2. The parameters of Pearson's ratio and Adj. R -square approximate to 1, suggesting a satisfactory linear relationship between the vertical load and deformation, especially the load deformation curve of the ISRFT with the least RSS.

Table 1 Fitting parameters of load deformation curves for NPMEW ($y=a \times x+b$)

Fitting parameter	RSS	Pearson's ratio	Adj. R -square	Intercept	Slope	$\sigma_{\text{Intercept}}$	σ_{Slope}
No.1	2.498 37	0.997 99	0.994 64	1.423 53	1.686 16	1.193 05	0.061 82
No.2	0.225 21	0.999 81	0.999 51	5.395 55	1.640 42	0.353 49	0.018 25

Table 2 Fitting parameters of load deformation curves for flexible tire body and ISRFT ($y=a \times x+b$)

Fitting parameter	RSS	Pearson's ratio	Adj. R -square	Intercept	Slope	$\sigma_{\text{Intercept}}$	σ_{Slope}
Flexible tire body	39.655 36	0.994 72	0.985 96	-1.636 97	7.446 84	3.065 68	0.443 53
ISRFT	0.645 15	0.999 38	0.998 34	0.280 11	2.306 11	0.674 79	0.046 98

The results indicate that it is accurate for the load deformation curves of the NPMEW and ISRFT by using the linear regression technology to fit. The average radial stiffness of the ISRFT is less than that of NPMEW, but larger than that of flexible tire body.

3.2 Static contact behavior

The NPMEW, considered as a sample, does not possess tread pattern in this experiment. Fig.12 shows the contact patch and contact pressure distribution of the longitudinal and lateral contact lengths, as a function of vertical loads. As demonstrated, the NPMEW contact patch is rectangular.

As the vertical load increases, the lateral contact length does not expand, and the contact length and area increase. Under small load, the contact pressure distribution in the longitudinal direction is similar to a parabola, and it demonstrates a local peak at the center of the contact patch. The contact pressure distribution along the lateral direction is similar to a rectangle, and the change of pressure value is small. The contact pressure along the longitudinal direction gradually expands as the vertical load increases, and the contact pressure also increases along the lateral direction. The shape of the lateral contact pressure profile is similar to the rectangular wave,

but the contact pressure demonstrates a local peak at the elastic ring of flexible tire body.

The contact patch and contact pressure distributions of the flexible tire body are shown in Fig.13, suggesting a similar distribution law to that of the NPMEW. The contact pressure distribution in the longitudinal direction is also similar to a parabola, and demonstrates the rectangle for lateral contact pressure profiles. The contact length and area of flexible tire body are larger than that of the NPMEW under the same vertical load.

The contact patch and contact pressure distributions of the ISRFT can be observed in Fig.14. The shape of contact patch is similar to an elliptical face when the vertical load and tire deformation are small. The longitudinal and lateral contact lengths gradually expand as the vertical load increases in the longitudinal and lateral directions. The contact pressure demonstrates a local peak in the middle of the

contact patch under small load, and it also gradually expands as the vertical load increases in every direction. In the center of the contact patch, the contact pressure distribution profile is similar to the saddle in the lateral direction, and to be flat in the longitudinal direction, and profile should be a curve on both sides. The results are consistent with Refs.[24-25]. The contact patch and contact pressure distributions of the ISRFT with rated filling pressure are same to that of conventional pneumatic tires. If tire pressure is sufficiently low so that the inner support body is in contact with the inside tread, the inner support will affect the pressure distribution. However, with the increase of load, the contact patch will warp, i. e., the pressure in the center of the contact area decreases, but the pressure on lateral sides increases, especially producing stress concentration phenomenon of the tire shoulder. Tire warping can accelerate tire wear and reduce tire service life^[26].

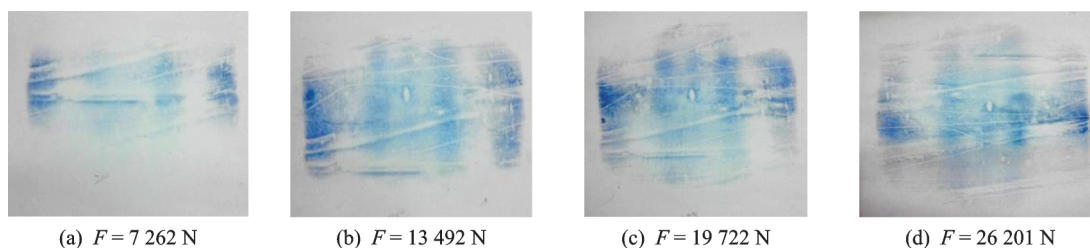


Fig.12 Static contact behavior of NPMEW

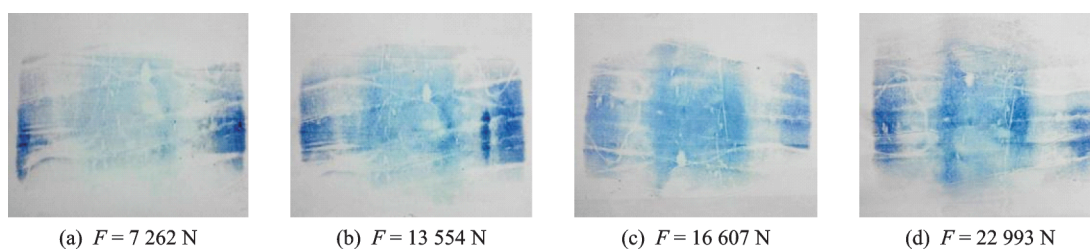


Fig.13 Static contact behavior of flexible tire body

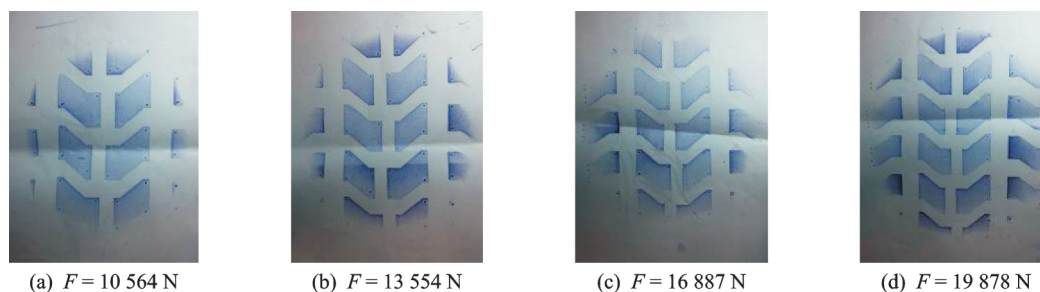


Fig.14 Static contact behavior of ISRFT

The contact behavior is evaluated using extracted geometrical and mechanical feature parameters, including longitudinal contact length L , lateral contact width W , contact behavior coefficient K (the ratio of longitudinal contact length and lateral contact width), contact area S , etc. Owing to the NPMEW with no tread pattern, the grounding area of the ISRFT here refers to the projected area of the tread surface on the rigid plane, rather than the contact area of the tread pattern to compare the two different tires. The mechanical characteristics of the contact behavior include hardness coefficient k , average pressure p , and pressure skewness value. The contact pressure distribution coordinate system is shown in Fig. 15, and the intersection point of axes X and Y is the geometric center of the contact patch.

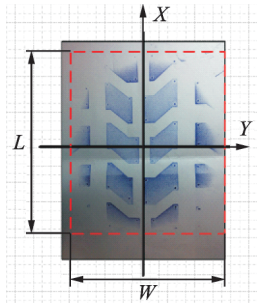


Fig.15 Contact pressure distribution coordinate system

The boundary of the contact patch is determined according to test results, and the characteristic parameters are calculated. Table 3 provides the characteristic parameters of contact pressure distribution for the NPMEW, flexible tire body, and ISRFT, respectively.

Statistics suggest that the lateral contact widths of the NPMEW and the flexible tire body indicate minimal change, and the longitudinal contact length, contact behavior coefficient, and contact area increases gradually with the increase of the load. The overall change trend indicates that the average contact pressure increases with the increase of the vertical load, reaching a certain peak value under the maximum load of 17 500 N, and subsequently it begins to decrease. Comparison of the contact pres-

Table 3 Characteristic parameters of contact behavior for three wheels

No.	NPMEW					
	F/N	W/mm	L/mm	K	S/mm^2	p/kPa
1	0	285	90	0.32	25 650	—
2	7 262	285	120	0.42	34 200	212.34
3	10 377	287	135	0.47	38 745	267.83
4	13 492	285	143	0.50	40 755	331.05
5	16 607	285	168	0.59	47 880	346.85
6	19 722	286	217	0.76	62 062	317.78
7	23 148	285	232	0.81	66 120	350.09
8	26 201	285	272	0.95	77 520	337.99
No.	Flexible tire body					
	F/N	W/mm	L/mm	K	S/mm^2	p/kPa
1	0	284	68	0.24	19 312	—
2	7 262	285	130	0.46	37 050	196.01
3	13 554	285	150	0.53	42 750	317.05
4	16 607	286	180	0.63	51 480	322.59
5	22 993	285	257	0.90	73 245	313.92
No.	ISRFT					
	F/N	W/mm	L/mm	K	S/mm^2	p/kPa
1	0	115	100	0.87	9 028	—
2	7 449	165	190	1.15	24 610	302.69
3	10 564	200	230	1.15	36 110	292.55
4	13 554	230	245	1.07	44 235	306.41
5	16 887	230	280	1.22	50 554	334.04
6	19 878	230	300	1.30	54 165	366.99

sure distribution characteristic parameters, the NPMEW and flexible tire body exhibit the same lateral contact width under the same load, but the longitudinal contact length, contact behavior coefficient, and contact area of flexible tire body are larger than those of the NPMEW.

The lateral contact width of the ISRFT increases with the increase in load, as illustrated in Table 3, and the value of the lateral contact width remain invariable after reaching 230 mm. The characteristic parameters of the longitudinal contact length, contact behavior coefficient, contact area, and average contact pressure increase with increasing vertical load.

Through comparison of characteristic parameters between NPMEW and ISRFT, the lateral contact width of NPMEW is larger than that of IS-

RFT, but the longitudinal contact length of NPMEW with high radial stiffness is less than that of ISRFT under the same section width and load.

When the load is less than maximum load, the contact area of ISRFT is larger than that of NPMEW. When the load is larger than the maximum load, the contact area of NPMEW is larger than that of ISRFT. From the perspective of average contact pressure, when the load is less than 13 500 N or larger than the maximum load, the average contact pressure of NPMEW is smaller than that of ISRFT. When the load ranges from 13 500 N to the maximum load, the average contact pressure of NPMEW is larger than that of ISRFT. The average contact pressure has a direct effect on the tire grip performance, and it is also an important factor regarding pavement damage. Excessively large average contact pressure will result in rapid tire wear.

To quantitatively analyze the uniformity of two tires, the pressure skewness value is used. It is defined as follows

$$\beta = \sqrt{\frac{1}{n_p - 1} \sum_{i=1}^{n_p} (p_i - p)^2}$$

where n_p is the sampling number, $n_p = 16$ in this study; p_i the contact pressure on sampling site No. i , and p the average contact pressure.

The pressure skewness value of NPMEW is calculated to be 165 kPa when the load is 19 700 N, and the pressure skewness value of ISRFT is 180 kPa, which is larger than that of NPMEW. The computed results indicate that NPMEW has more uniform contact pressure distribution than ISRFT under 19 700 N.

Based on the above analysis, the NPMEW demonstrates more uniform contact pressure than ISRFT within a certain loading range, and it can efficiently mitigate the problem of stress concentration in ISRFT shoulder under heavy load and enhance the wear resistance and ground grip performances.

4 Conclusions

A non-pneumatic mechanical elastic wheel is investigated as a function of static radical stiffness characteristics and contact behavior using bench test method. The load deformation curves of the NPMEW and ISRFT indicate a satisfactory linear relationship between the vertical load and deformation within the scope of applied load. The NPMEW has higher radical stiffness than that of the ISRFT, which is larger than that of the flexible tire body in this study. The value of radical stiffness for NPMEW is dependent on the mechanical characteristic of flexible tire body and hinge units. To replace the pneumatic tire, the NPMEW stiffness characteristics require further optimizing and matching with the suspension system and the entire vehicle dynamics parameters.

The tread contact stiffness distribution of the NPMEW is improved through suspension hub loaders, and it can efficiently mitigate the problem of stress concentration in ISRFT shoulder under heavy load and enhance the wear resistance and ground grip performances. The lateral contact width of NPMEW is larger than that of ISRFT, but the longitudinal contact length of NPMEW with high radial stiffness is less than that of ISRFT under the same load.

References

- [1] GENT A N, WALTER J D. The pneumatic tire[M]. Washington DC: National Highway Traffic Safety Administration, 2005.
- [2] PACEJKA H B. Tyre and vehicle dynamics[M]. Burlington: Butterworth-Heinemann, 2006.
- [3] KWANGWON K, JAEHYUNG J, DOO M K. Static contact behaviors of a non-pneumatic tire with hexagonal lattice spokes[J]. SAE International Journal of Passenger Cars-Mechanical Systems, 2013, 6(3): 1518-1527.
- [4] JULIEN C, FABIENNE A, DENIS D, et al. Experimental study of tyre/road contact forces in rolling conditions for noise prediction[J]. Journal of Sound and Vibration, 2009, 320: 125-144.

- [5] JAEHYUNG J, BALAJEE A, JOSHUA D S, et al. Design of cellular shear bands of a non-pneumatic tire-investigation of contact pressure[J]. *SAE International Journal of Passenger Cars-Mechanical Systems*, 2010, 3(1): 598-606.
- [6] RHYNE T B, CRON S M. Development of a non-pneumatic wheel[J]. *Tire Science and Technology*, 2006, 34(3): 150-169.
- [7] JAEHYUNG J, DOO M K, KWANGWON K. Flexible cellular solid spokes of a non-pneumatic tire[J]. *Composite Structures*, 2012, 94: 2285-2295.
- [8] IN G J, YOUNG H S, EUI J Y, et al. Pattern design of a non-pneumatic tyre for stiffness using topology optimization[J]. *Engineering Optimization*, 2012, 44(2): 119-131.
- [9] SHASHANK B. Design and analysis of alternating spoke pair concepts for a non-pneumatic tire with reduced vibration at high speed rolling[D]. Clemson, USA: Clemson University, 2009.
- [10] ZHAO Y Q, ZANG L G, CHEN Y Q, et al. Non-pneumatic mechanical elastic wheel natural dynamic characteristics and influencing factors[J]. *Journal of Central South University*, 2015, 22(5): 1707-1715.
- [11] ZANG L G, ZHAO Y Q, LI B, et al. An experimental study on the ground contact characteristics of non-pneumatic mechanical elastic wheel[J]. *Automotive Engineering*, 2016, 38(3): 350-355.
- [12] ZANG L G, ZHAO Y Q, LI B, et al. Mechanical elastic wheel improving road holding and wear resistance of tire[J]. *Transactions of the Chinese Society of Agricultural Engineering (Transactions of the CSAE)*, 2014, 30(12): 56-63.
- [13] KATO K, YAMAGUCHI M, MIYAZONO T, et al. Enhancement of tire durability by considering air flow field[J]. *Tire Science and Technology*, 2009, 37(2): 103-121.
- [14] CHO J R, LEE J H, JEONG K M, et al. Optimum design of run-flat tire insert rubber by genetic algorithm[J]. *Finite Elements in Analysis and Design*, 2012, 52: 60-70.
- [15] LI B, ZHAO Y Q, ZANG L G, et al. Driving force model for non-pneumatic elastic wheel[J]. *Transactions of Nanjing University of Aeronautics and Astronautics*, 2016, 33(2): 231-236.
- [16] DENG Y J, ZHAO Y Q, LIN F, et al. Simulation of steady-state rolling non-pneumatic mechanical elastic wheel using finite element method[J]. *Simulation Modelling Practice and Theory*, 2018, 85: 60-79.
- [17] FU H X, ZHAO Y Q, LIN F, et al. Steady-state cornering properties of a non-pneumatic tire with mechanical elastic structure[J]. *Transactions of Nanjing University of Aeronautics and Astronautics*, 2017, 34(5): 586-592.
- [18] ZHAO Y Q, DENG Y J, LIN F, et al. Transient dynamic characteristics of a non-pneumatic mechanical elastic wheel rolling over a ditch[J]. *International Journal of Automotive Technology*, 2018, 19(3): 499-508.
- [19] DU X B, ZHAO Y Q, WANG Q, et al. Numerical analysis of the dynamic interaction between a non-pneumatic mechanical elastic wheel and soil containing an obstacle[J]. *Proceedings of the Institution of Mechanical Engineers, Part D: Journal of Automobile Engineering*, 2017, 231(6): 731-742.
- [20] DU X B, ZHAO Y Q, LIN F, et al. Numerical and experimental investigation on the camber performance of a non-pneumatic mechanical elastic wheel[J]. *Journal Brazilian Society of Mechanical Sciences & Engineering*, 2017, 39: 3315-3327.
- [21] LI B, ZHAO Y Q, ZANG L G, et al. Closed-form solution of curved beam model of elastic mechanical wheel[J]. *Journal of Vibroengineering*, 2014, 16(8): 3951-3962.
- [22] YUE H X, ZHAO Y Q. Nonlinear finite element analysis of a new safety wheel[J]. *China Mechanical Engineering*, 2012, 23(11): 1380-1385.
- [23] ZANG L G, ZHAO Y Q, LI B, et al. Static and dynamic characteristics of local-damaged mechanical elastic tire[J]. *Journal of Vibration, Measurement & Diagnosis*, 2016, 36(3): 478-483.
- [24] ZHUANG J D. *Advanced technology of tire*[M]. Beijing: Beijing Institute of Technology Press, 2001.
- [25] LIANG C, WANG G L, ZHOU H C, et al. Experimental study of radial tire contact pressure distribution evaluation[J]. *Automobile Technology*, 2013, 11: 38-42.
- [26] KIM S M, DARABI M K, LITTLE D N, et al. Effect of the realistic tire contact pressure on the rutting performance of asphaltic concrete pavements[J]. *Mechanistic Evaluation of Asphalt Paving Materials and Structures*, 2018, 22(6): 2138-2146.

Acknowledgements This work was supported in part by the National Natural Science Foundations of China (Nos.

51605215, 11672127), the National Science Foundations for Post-Doctoral Scientists of China (Nos.2018M630593, 2019T120450), Research Foundations of Nanjing Institute of Technology (Nos. QKJ201707, PTKJ201702), and the Qing Lan Project.

Authors Dr. ZANG Liguó received the B.S. degree in automotive engineering from Shandong University of Technology in 2008 and the Ph.D. degree in automotive engineering from Nanjing University of Aeronautics and Astronautics (NUAA) in 2015, respectively. He joined in Nanjing Institute of Technology in July 2015. His research has focused on vehicle system dynamics, safety tire theory and technology.

Prof. ZHAO Youqun received the B.S. degree in engineering mechanics from Jilin University in 1990 and the Ph.D. degree in automotive engineering from Jilin University in 1998, respectively. In 2011, she joined College of Energy and Power Engineering, NUAA, Nanjing, China.

Ms. SUN Haiyan received the B.S. degree in traffic engi-

neering from Shandong University of Technology in 2008 and the M.S. degree in vehicle operation engineering from Jilin University in 2012, respectively. He joined Nanjing Institute of Technology in September 2016. Her research focuses on intelligent vehicle technology.

Prof. LIN Fen received the B.S. and Ph.D. degrees in automotive engineering from NUAA in 2002 and 2008, respectively. In 2009, he joined College of Energy and Power Engineering, NUAA, Nanjing, China.

Author contributions Dr. ZANG Liguó designed the study, conducted the analysis, interpreted the results and wrote the manuscript. Prof. ZHAO Youqun contributed to the discussion and background of the study. Ms. SUN Haiyan contributed to data for the analysis of static radical stiffness and contact behavior. Prof. LIN Fen contributed to the discussion and background of the study.

Competing interests The authors declare no competing interests.

(Production Editor: Xu Chengting)